Characteristic Model Based All-coefficient Adaptive Control of a Flexible Rotor Suspended on Active Magnetic Bearings

Long Di, Simon E. Mushi, Zongli Lin, Paul E. Allaire
University of Virginia
Charlottesville, VA 22904, USA
{ld4vv,sem5t,zl5y,pea}@virginia.edu

Abstract

Active magnetic bearings (AMBs) have been used in many high-speed rotating machinery applications. Because of the nonlinear characteristics of magnetic bearings and complex dynamics of the flexible rotors, the problems of stabilization and disturbance rejection need to be extensively addressed for their smooth operation over a wide operating speed range. Conventional controller such as the proportional-integral-derivative (PID) design has played a major role in most AMB related applications. Although it is easy to implement, there exist limitations and drawbacks. The μ-synthesis approach can fulfill the requirement of robust performance, but it relies on the plant and uncertainty models, which are sometimes difficult to acquire for practical systems. This paper explores the use of the characteristic model based all-coefficient adaptive control (ACAC) method to stabilize a flexible rotor AMB system. This new control method does not require an actual model of the system. Both simulation and experimental results have shown its strong potential to perform well in spite of its simplicity.

1 Introduction

Active magnetic bearings are becoming popular in practical applications and have been an active research subject for years. Compared with conventional mechanical bearings, AMBs operate quite differently in many prospectives. On one hand, AMBs rely on electromagnetic force to support the object, and there is no physical contact, creating an operation environment nearly free of friction. On the other hand, AMBs require feedback control to generate appropriate supporting force, which demands additional electronic devices. Although AMBs possess several advantages such as higher efficiency and reliability, lower maintenance and repairing cost, and clean working environment, they also reveal more complexities since they require auxiliary equipments to provide the desired control performance. Because of the nonlinearity and instability of AMBs, controller design is the most essential task in an AMB system.

Currently PID controllers are the most widely used control mechanism for magnetic bearing related industrial applications [1]. Because of their simplicity, they are easy to implement and with intuitive tuning process, they can achieve reasonable control performance. However, for complex dynamic systems, it is difficult for those controllers to deliver robust and near optimal performance. In recent years, robust control techniques such as μ-synthesis have also been applied to magnetic bearing applications [2, 3]. Compared with PID control, the μ-synthesis approach is able to better handle the uncertainties in complex system and achieve reliable performance. However, μ-synthesis needs the plant and uncertainty models to generate the most suitable solution, and in reality, it takes a lot of efforts to model a complex system. Besides, if the properties of the plant change significantly, the original μ controller might not work properly anymore.

Characteristic model based all-coefficient adaptive control (ACAC) method has been widely used in process control and aerospace industry, and numerous application examples have demonstrated its effectiveness [4]. This method is able to provide robust control performance on multi-dimensional complex dynamical systems, while maintaining a simple structure and not requiring the

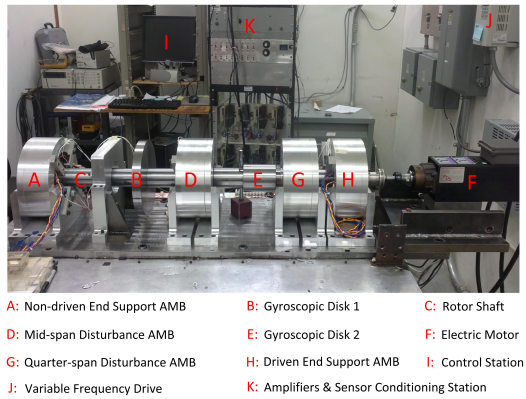

Figure 1: Test rig overview.

actual plant model [5–7]. This paper explores using the characteristic model based ACAC method to stabilize a flexible rotor AMB test rig.

This paper is organized as follows. Section 2 describes the flexible rotor AMB test rig, the principle of AMB control and an existing μ-synthesis controller. In Section 3, the concept of characteristic modeling and the all-coefficient adaptive control mechanism are introduced. Section 4 presents the implementation and shows the simulation and experimental results. Conclusions are drawn in Section 5.

2 A System Description

2.1 The Test Rig

The AMB test rig [8] was designed and built as a research platform in the Rotating Machinery and Controls (ROMAC) Laboratory at University of Virginia. The original purpose of this test rig is to emulate an industrial centrifugal gas compressor and study control of the rotordynamic instability. The rotor is 1.23 m long and weighs around 44.9 kg. Four laminated steel journals are mounted on the shaft for two radial support AMBs at the nondriven end (NDE) and driven end (DE), and two radial disturbance AMBs at the middle and quarter span. Only the NDE and DE support AMBs are utilized for control. There are also two auxiliary ball bearings mounted at the support AMB locations to prevent damage to AMBs when the rotor drops. A 3.7 kW Colombo RS-90/2, electric fan cooled, high speed motor with variable frequency drive (VFD) is used to make the rotor run up to 18,000 rpm, and a 2.2 Nm motor torque is also available for this speed.

Four amplifiers are installed for each radial magnetic bearing and each amplifier features a 25 kHz switching frequency. The maximum continuous current rates at 10 A, which gives each AMB a static load capacity of 1450 N. The rotor motion is monitored by a 10 channel Kaman eddy current sensor system and the displacement of each control axis is measured by a 1H/15N static probe. The digital control system is based on the Innovative Integration M6713 PCI board and a TI C6713B 32-bit floating point digital signal processing (DSP) chip is used for the implementation of the digital control algorithm with an updating frequency around 12 kHz. There are 16 channels of analog input and output to be simultaneously sampled and interfaced with the actuators and sensors. A control station computer with custom graphic user interface is also designed to provide the user with many functionalities. The entire AMB test rig system is shown in Fig. 1.

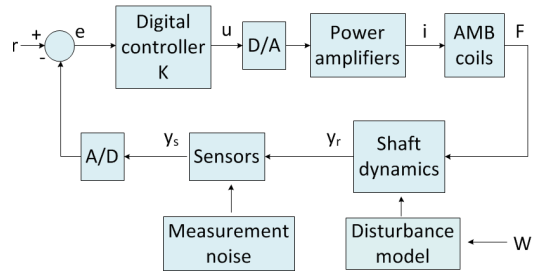

Figure 2: AMB control flow diagram.

2.2 AMB Control

Closed-loop feedback control is critical for the stabilization of an AMB system. The μ-synthesis approach is applied to the AMB control design using Matlab function dksyn for D-K iteration with 4 iterations to find the reasonable μ value [9]. The final μ-synthesis design is a 48th order controller with $\mu = 0.856$ for the plant model of 48 states, which include models of the rotor dynamics, AMBs, sensors, amplifiers and other components. In Simulink, it is implemented in a state space form for the x and y axes of both DE and NDE [3]. This design is later implemented in a DSP computer and the performance requirement and parametric uncertainties of the rotor-AMB system have been well handled by the μ-synthesis control [9].

A typical control flow diagram consisting of the major components, including controller, AMB coils, shaft and sensors, is shown in Fig. 2. In this diagram, r is the reference signal, e is the error signal, u is the controller output, i is the control current, F is the AMB force, y_r is the shaft displacement, y_s is the position sensor reading and W is the external disturbance force.

3 Characteristic Model Based All-coefficient Adaptive Control

3.1 Characteristic Modeling

This modeling process focuses on the characteristics of the plant and the control performance requirement instead of precise system dynamics. It compresses the corresponding information of the high order plant into several characteristic parameters. The characteristic model remains a simple structure but it closely reflects the feature of the original system. A linear time-invariant plant can be described as

$$G(s) = \frac{b_m s^m + b_{m-1} s^{m-1} + \cdots + b_1 s + b_0}{s^n + a_{n-1} s^{n-1} + \cdots + a_1 s + a_0}. \tag{1}$$

It has been established in [4] that this linear time invariant plant (1) can be represented by a time-varying difference equation of a lower order. The exact order of this difference equation is determined by the control objective. For our approach, we recall the following results.

Consider a linear time-invariant plant as given by (1). If the control objective is position keeping or tracking, then, for a small enough sampling period T, the characteristic model is a second-order time-varying difference equation,

$$y(k) = f_1(k)y(k-1) + f_2(k)y(k-2) + g_0(k)u(k-1) + g_1(k)u(k-2), \tag{2}$$

where $u(k)$ and $y(k)$ are respectively the control input and the system output at the kth sampling point.

The characteristic model (2) possesses the following properties:

- Coefficients $f_1(k)$, $f_2(k)$, $g_0(k)$ and $g_1(k)$ are slowly time varying.
- The ranges of these parameters can be decided *a priori*.
- In response to a same input, the output of the original model (1) and that of the characteristic model (2) are identical at the sampling points.
- Assume that the static gain of system (1)

$$D = G(0) = \frac{b_0}{a_0} = 1.$$

Then the sum of all the coefficients approaches 1, *i.e.*,

$$f_1(\infty) + f_2(\infty) + g_0(\infty) + g_1(\infty) = 1.$$

3.2 All-coefficient Adaptive Control

The all-coefficient adaptive control has been widely used in many engineering applications with stable and robust control performance [10]. Consider a linear time-invariant plant

$$y^{(n)} = a_{n-1}y^{(n-1)} + \cdots + a_0 y + b_{n-1}u^{(n-1)} + \cdots + b_0 u,$$

whose discretized equation is written as

$$y(k) = \alpha_1 y(k-1) + \alpha_2 y(k-2) + \cdots + \alpha_n y(k-n) + \beta_0 u(k) + \cdots + \beta_{n-1}u(k-n+1). \tag{3}$$

The coefficients of (3) satisfy the following conditions [4]:

- If the static gain D equals to unity, then the sum of all the coefficients equals to one,

$$\sum_{i=1}^{n} \alpha_i + \sum_{i=0}^{n-1} \beta_i = 1.$$

- If the static gain $D \neq 0$ and is bounded, then the sum of all the coefficients approaches one as $T \to 0$, *i.e.*,

$$\lim_{T\to 0} \left(\sum_{i=1}^{n} \alpha_i + \sum_{i=0}^{n-1} \beta_i \right) = 1.$$

The ranges of α_i and β_i can be determined in advance based on the ranges of a_i and b_i, and the value of sampling time T, which is usually chosen as

$$T \in \left[\frac{T_{\min}}{15}, \frac{T_{\min}}{3} \right],$$

where $T_{\min}$ is the minimum equivalent time constant of the system and it can be measured in practical applications.

Once the ranges of the parameters are specified, parameter estimates should not only rely on the algorithm of the parameter estimation, but also satisfy the requirements that they are constrained by closed sets and the sum of all coefficients should equal to one. The initial values of those coefficients are chosen from the specified closed sets, so the estimated parameters can more closely approach their actual values, which will improve the performance of the adaptive control during the transient process.

The difference equation (3) can be written in the following compact form to facilitate parameter estimation,

$$y(k) = \phi^T(k)\theta + \beta_0 u(k),$$

where $\phi(k)$ and θ are defined as

$$\begin{aligned}\phi(k) &= [y(k-1)\ \ y(k-2)\ \ \cdots\ \ y(k-n)\ \ u(k-1)\ \ u(k-2)\ \ \cdots\ \ u(k-n+1)]^T,\\ \theta &= [\alpha_1\ \ \alpha_2\ \ \cdots\ \ \alpha_n\ \ \beta_1\ \ \beta_2\ \ \cdots\ \ \beta_{n-1}]^T.\end{aligned}$$

Let the feedback control $u(k)$ be given as

$$u(k) = -\phi^T(k)L(k),$$

where $L(k) = [L_1(k), L_2(k), \cdots, L_{2n-1}(k)]$ is a feedback gain that makes the closed-loop system stable.

We can adopt a least-squares algorithm to update $\hat{\theta}(k)$ as follows [11],

$$\begin{aligned}P(k) &= P(k-1) - \frac{P(k-1)\phi(k)\phi^T(k)P(k-1)}{\lambda + \phi^T(k)P(k-1)\phi(k)},\\ \hat{\theta}(k) &= \hat{\theta}(k-1) + \beta_0(k)L(k) - \beta_0(k-1)L(k-1)\\ &\quad + P(k)\phi(k)[y(k) - \phi^T(k)(\hat{\theta}(k-1) - \beta_0(k-1)L(k-1))].\end{aligned} \tag{4}$$

In order to update $\hat{\beta}_0$, based on the fact that the sum of all the coefficients equals to 1, it follows from (4) that [11],

$$\hat{\beta}_0(k) = \hat{\beta}_0(k-1) - \frac{\theta_s + \hat{\beta}_0(k-1) - 1}{L_s + 1} - MP(k)\phi(k)\frac{y(k) - \phi(k)^T[\hat{\theta}(k-1) - \hat{\beta}_0(k-1)L(k)]}{L_s + 1},$$

where θ_s, L_s and M are given as

$$\begin{aligned}\theta_s &= \sum_{i=1}^{2n-1} \theta_i(k-1),\\ L_s &= \sum_{j=1}^{2n-1} L_j(k),\\ M &= [\underbrace{1\ 1\cdots 1}_{2n-1}\ \underbrace{0\ 0\cdots 0}_{n}].\end{aligned}$$

The all-coefficient adaptive control $u(k)$ generally consists of a maintaining/tracking control $u_m(k)$, a golden section feedback control $u_f(k)$, a logic differential control $u_d(k)$ and a logic integral control $u_i(k)$. It can be written as

$$u(k) = u_m(k) + u_f(k) + u_d(k) + u_i(k),$$

where $u_m(k)$, $u_f(k)$, $u_d(k)$ and $u_i(k)$ are respectively specified as

1. Maintaining/tracking control

$$u_m(k) = \frac{y_r(k) - \phi^T(k)\hat{\theta}(k)}{\hat{\beta}_0(k)},$$

where $y_r(k)$ is the desired output;

2. Golden section feedback control

$$u_f(k) = \frac{l_1\hat{\alpha}_1(k)\tilde{y}(k) + l_2\hat{\alpha}_2(k)\tilde{y}(k-1)}{\hat{\beta}_0(k)},$$

where $l_1 = 0.382$, $l_2 = 0.618$, $\hat{\alpha}_1(k)$ and $\hat{\alpha}_2(k)$ are the estimates of α_1 and α_2, and $\tilde{y}(k) = y_r(k) - y(k)$;

3. Logical differential control

$$u_d(k) = k_1\frac{\tilde{y}(k) - \tilde{y}(k-1)}{T},$$
$$k_1 = k_d\sqrt{\sum_{i=1}^{N}[\mid \tilde{y}(k-N+i) - \tilde{y}(k-N+i-1) \mid]},$$

where k_d is a positive constant;

4. Logical integral control

$$u_i(k) = u_i(k-1) + k_2\tilde{y}(k),$$
$$k_2 = \begin{cases} k_{i1}, & \tilde{y}(k)[\tilde{y}(k) - \tilde{y}(k-1)] - \psi \le 0, \\ k_{i2}, & \tilde{y}(k)[\tilde{y}(k) - \tilde{y}(k-1)] - \psi > 0, \end{cases}$$

where k_{i2}, k_{i1} and ψ are all positive constants with $k_{i2} > k_{i1}$ and ψ being a small number.

3.3 Characteristic Model Based All-coefficient Adaptive Control

The characteristic model (2) can be written as follows to facilitate parameter estimation,

$$y(k) = \phi^T(k-1)\theta(k),$$

where $\phi(k-1)$ and $\theta(k)$ are defined as

$$\phi(k-1) = [y(k-1) \quad y(k-2) \quad u(k-1) \quad u(k-2)]^T,$$
$$\theta(k) = [f_1(k) \quad f_2(k) \quad g_0(k) \quad g_1(k)]^T.$$

In order to specify the ranges of the parameters, we first analyze a second order time-invariant difference equation as

$$y(k) = \alpha_1 y(k-1) + \alpha_2 y(k-2) + \beta_0 u(k-1) + \beta_1 u(k-2).$$

The ratio between the sampling time T and the minimum equivalent time constant $T_{\min}$ satisfies $\frac{T}{T_{\min}} = \eta \in [0, \eta_{\max}]$ and the ratio between T and the maximum equivalent time constant $T_{\max}$ satisfies $\frac{T}{T_{\max}} \in [0, \eta]$.

According to [11], when $\eta_{\max} \leq \frac{1}{3}$, the parameters satisfy the following conditions for unstable plants:

$$\begin{cases} 2\cos(\frac{\eta_{\max}}{2}) \leq \alpha_1 \leq 2e^{\frac{\eta_{\max}}{2}}, \\ -e^{\eta_{\max}} < \alpha_2 \leq -1, \\ 2e^{\frac{\eta_{\max}}{2}}\cos(\frac{\eta_{\max}}{2}) - e^{\eta_{\max}} \leq \alpha_1 + \alpha_2 < -1, \\ \frac{b_0 T^2}{2} < \beta_0 < \frac{b_0 T^2}{2}(1+\frac{\eta_{\max}}{3}+\frac{\eta_{\max}^2}{12}), \\ \frac{b_0 T^2}{2}(1-\frac{\eta_{\max}^2}{24}) < \beta_1 < \frac{b_0 T^2}{2}(1+\frac{2\eta_{\max}}{3}+\frac{7\eta_{\max}^2}{24}). \end{cases}$$

Based on the conditions above, it can be observed that $\alpha_1 \to 2$, $\alpha_2 \to -1$, $\beta_0 \to 0$, $\beta_1 \to 0$, as $T \to 0$. Let

$$\begin{cases} \frac{T}{T_{\min}} \in [\frac{1}{10}, \frac{1}{4}], \\ \frac{T}{T_{\max}} \in [0, \frac{1}{10}]. \end{cases}$$

Then the ranges for the corresponding parameters can be calculated with $\eta_{\max} = \frac{1}{4}$ [11],

$$\begin{cases} \alpha_1 \in [1.9844, 2.2663], \\ \alpha_2 \in [-1.2840, -1], \\ \alpha_1 + \alpha_2 \in [0.9646, 1]. \end{cases}$$

Because β_0 and β_1 are close to 0, we can choose some really small positive numbers for $g_0(k)$ and $g_1(k)$. For the stability of the system, $f_1(k)$ and $f_2(k)$ are to be chosen from

$$N = \{(f_1(k), f_2(k)) \mid 1.9844 < f_1(k) < 2.2663, -1.2840 < f_2(k) < -1\}.$$

Let $\hat{\theta}(k)$ be the estimate of the parameter vector $\theta(k)$. Then the estimation error $\varepsilon(k)$ is

$$\varepsilon(k) = y(k) - \phi^T(k-1)\hat{\theta}(k) = (\theta(k) - \hat{\theta}(k))^T \phi(k-1).$$

We can adopt the gradient adaptive law and a direct mapping approach to acquire $\hat{\theta}(k)$,

$$\hat{\theta}_u(k+1) = \hat{\theta}(k) + \frac{\gamma\phi(k)\varepsilon(k)}{\delta + \phi^T(k)\phi(k)},$$
$$\hat{\theta}(k+1) = \pi[\hat{\theta}_u(k+1)],$$

where $\delta \geq 0$, $0 < \gamma < 2$, and $\pi[x]$ is the projection of x into N [12].

The characteristic model based all-coefficient adaptive control scheme $u_c(k)$ for the AMB control is written as

$$u_c(k) = u_{c1}(k) + u_{c2}(k) + u_{c3}(k) + u_{c4}(k),$$

where $u_{c1}(k)$, $u_{c2}(k)$, $u_{c3}(k)$ and $u_{c4}(k)$ are respectively specified as

1. Maintaining/tracking control

$$u_{c1}(k) = \frac{y_r(k) - \hat{f}_1(k)y(k) - \hat{f}_2(k)y(k-1) - \hat{g}_1(k)u_{c1}(k-1)}{\hat{g}_0(k) + \lambda_1},$$

where $y_r(k)$ is the desired output, λ_1 is a positive constant, and $\hat{g}_0(k)$, $\hat{f}_1(k)$, $\hat{f}_2(k)$ and $\hat{g}_1(k)$ are the estimates of $g_0(k)$, $f_1(k)$, $f_2(k)$ and $g_1(k)$, respectively;

2. Golden section adaptive control

$$u_{c2}(k) = \frac{l_{c1}\hat{f}_1(k)\tilde{y}(k) + l_{c2}\hat{f}_2(k)\tilde{y}(k-1) + \hat{g}_1(k)u_{c2}(k-1)}{\hat{g}_0(k) + \lambda_1},$$

where $\tilde{y}(k) = y_r(k) - y(k)$, $l_{c1} = 0.382$ and $l_{c2} = 0.618$;

3. Differential control

$$u_{c3}(k) = d_1 \frac{\tilde{y}(k) - \tilde{y}(k-1)}{T},$$

where d_1 is a positive constant;

4. Integral control

$$u_{c4}(k) = d_2 \sum_{i=1}^{k} \tilde{y}(i) = u_{c4}(k-1) + d_2\tilde{y}(k),$$

where d_2 is a positive constant.

4 Simulation and Experimental Results

In order to verify the proposed ACAC design, both simulation and experimental studies have been conducted. The simulation is based on the Simulink model derived for the entire rotor AMB system, which includes all essential components of the test rig. The μ-synthesis controller was initially used to stabilize the test rig and its performance serves as a baseline for comparison with our characteristic model based all-coefficient adaptive controller. To verify the characteristic model based ACAC approach, the original μ-synthesis controller in Simulink is replaced by the ACAC mechanism. For the x and y axes at both driven and nondriven ends, ACAC with the same controller parameters are utilized.

The simulation results are illustrated in Figs. 3 and 4. In the simulation, $f_1(0) = 2.102$, $f_2(0) = -1.104$ and $g_0(0) = g_1(0) = 0.001$. Note that

$$f_1(0) + f_2(0) + g_0(0) + g_1(0) = 1.$$

The controller parameters are chosen as $\lambda_1 = 0.16$, $d_1 = 0.0257$, $d_2 = 0.01$, $\delta = 3.5$ and $\gamma = 1.5$. The test starts with rotating speed at 0 rpm and goes up to 14400 rpm. It can be noticed that for different control channels, the control signals of ACAC are very similar due to the same coefficient settings, while for the μ-synthesis, the control signals vary for different channels. In terms of the vibrations at both driven and nondriven ends, it can be observed that the displacements of x and y axes under control of ACAC are much smaller than those using μ-synthesis for most of the speed range. The parameter estimations are shown in Fig. 5, where with the change of the rotating speed, the controller parameters also get updated accordingly to guarantee stable control performance.

We next implemented the ACAC algorithm on a DSP computer for the actual AMB test rig to verify the simulation results. The same initial conditions and controller parameters as used in

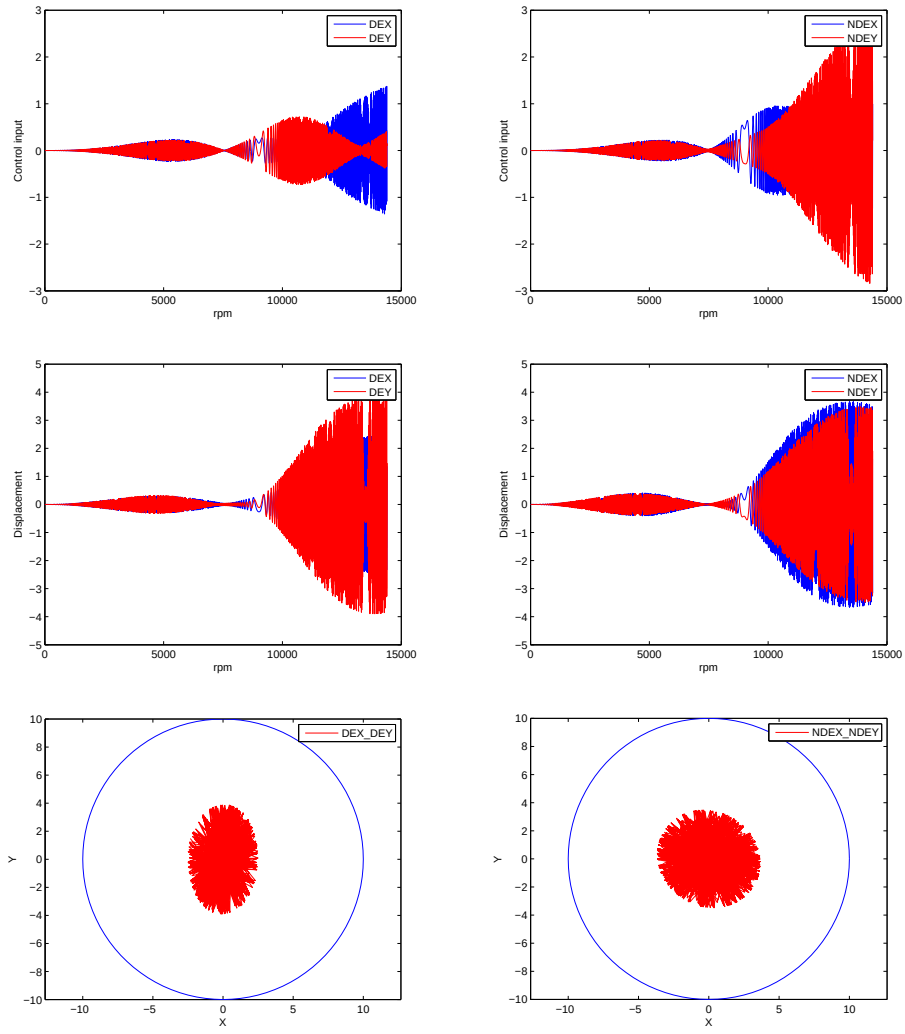

Figure 3: μ-synthesis simulation results (control inputs, shaft displacements and orbit size).

simulation are applied in the experiment. For practical implementation purpose, a first order low-pass filter combined with a phase bump filter is designed to roll off the high frequency gains [13]. A notch filter is also added to attenuate the noise effect caused by the second bending mode [14], which is around 530 Hz. The original ACAC algorithms get converted to C code and replace the existing μ-synthesis algorithm. The recorded highest rotating speed is around 14400 rpm at which the rotor remains stable. ACAC approach preserves reliable performance and is comparable to the μ-synthesis in certain measures, as shown in Figs. 6 and 7. It can be observed that for both ACAC method and μ-synthesis, the control signals have several peaks when the rotor passes through the rigid body modes and move towards the first bending mode. The control voltage of μ-synthesis is smaller than the ACAC method and it also has a narrower bandwidth, which causes the operation to be quieter. In terms of vibration attenuation, the ACAC method is more effective in both driven and nondriven ends by generating smaller rotating circles within 1.8 mils.

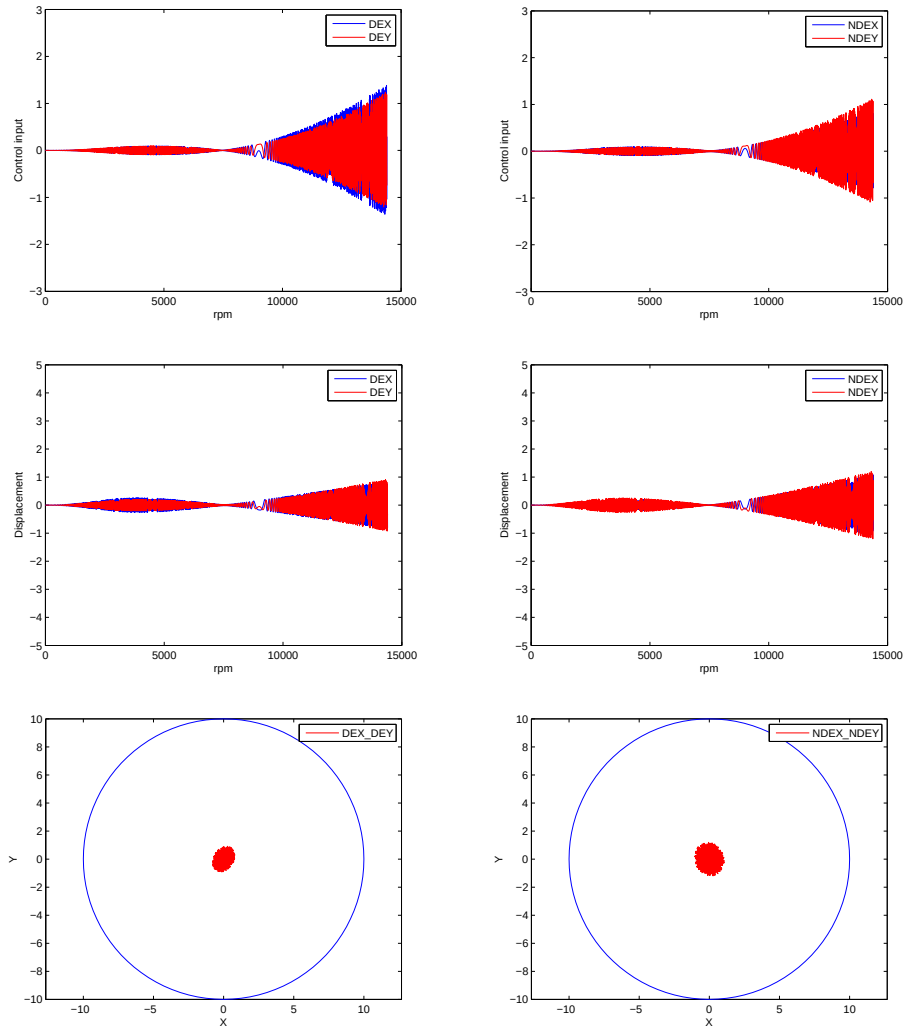

Figure 4: ACAC simulation results (control inputs, shaft displacements and orbit size).

5 Conclusions

This paper presents applying characteristic model based all-coefficient adaptive control on a flexible rotor AMB system. The nonlinearity, uncertainty and high order natures of flexible rotor AMB systems cause challenges for control system design. Although μ-synthesis is able to sufficiently meet these challenges in a robust manner, it requires the plant and uncertainty models and the actual controller is quite complex, which might not be convenient for practical applications. The characteristic modeling method significantly simplifies the modeling of a complex dynamical system by analyzing its characteristics and considering the control requirement. Based on this method, we can use a second order time-varying difference equation to handle a position tracking/keeping scenario. The resulting characteristic model based all-coefficient adaptive control design adopts a modified gradient adaptive law. Both the simulation studies and experimental results of the ACAC approach

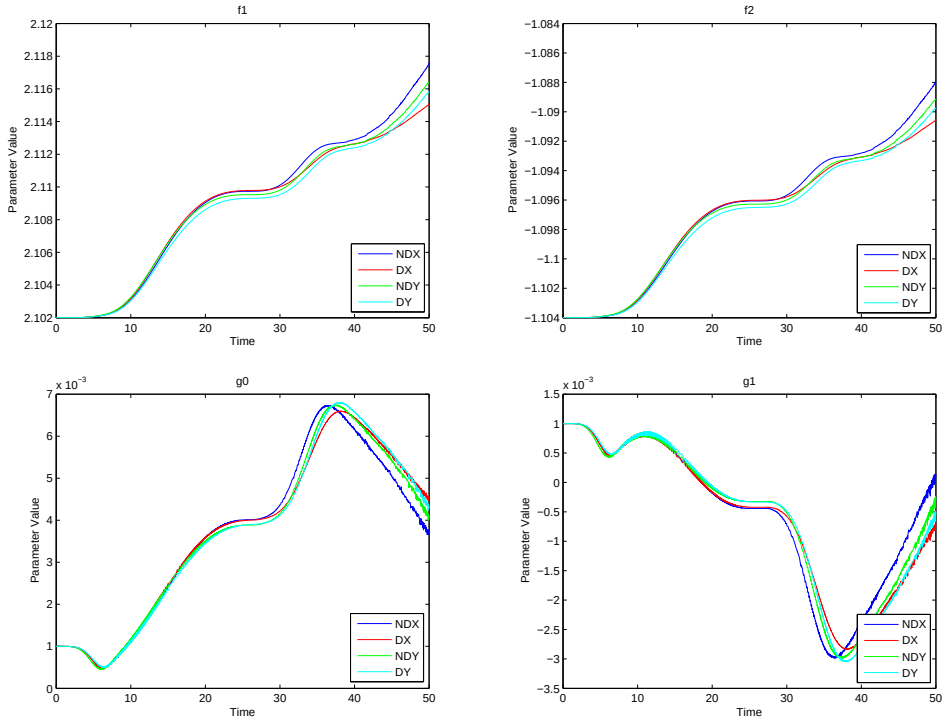

Figure 5: Estimation of parameters $f_1(k)$, $f_2(k)$, $g_0(k)$ and $g_1(k)$.

have shown the effectiveness of this design method and its strong potentials.

References

[1] G. Schweitzer and E. H. Maslen. *Magnetic Bearings*. Springer, 2009.

[2] E. H. Maslen and J. T. Sawicki. Mu-synthesis for magnetic bearings: Why use such a complicated tool? In *Proc. of the ASME 2007 Int. Mech. Eng. 843 Cong. and Expo. (IMECE'07)*, page 1103–1112, Seattle, Washington, 2007.

[3] S. E. Mushi, Z. Lin, and P. E. Allaire. Design, construction, and modeling of a flexible rotor active magnetic bearing test rig. *IEEE/ASME Trans. Mechatronics*, PP(99):1–13, 2011.

[4] H. Wu, J. Hu, and Y. Xie. Characteristic model-based all-coefficient adaptive control method and its applications. *IEEE Trans. Systems, Man, and Cybernetics, Part C: Applications and Reviews*, 37(2):213–221, 2007.

[5] H. Wu, Y. Liu, Z. Liu, and Y. Xie. Characteristic modeling and the control of flexible structure. *Science in China Series: Information Sciences*, 44(4):278–291, 2001.

[6] G. Zhang, J. Liu, and H. Wu. Adaptive control of large flexible structures using the characteristic modeling technique. In *Proc. of IMACS Multiconference on "Computational Engineering in Systems Applications"(CESA)*, Beijing, China, Oct. 4-6, 2006.

[7] Z. Li, Z. Wang, and J. Li. A hybrid control scheme of adaptive and variable structure for flexible spacecraft. *Aerospace Science and Technology*, 8:423–430, 2004.

[8] S. E. Mushi. Control of flexible rotors supported by active magnetic bearings. Master's thesis, Univ. of Virginia, Charlottesville, VA, 2008.

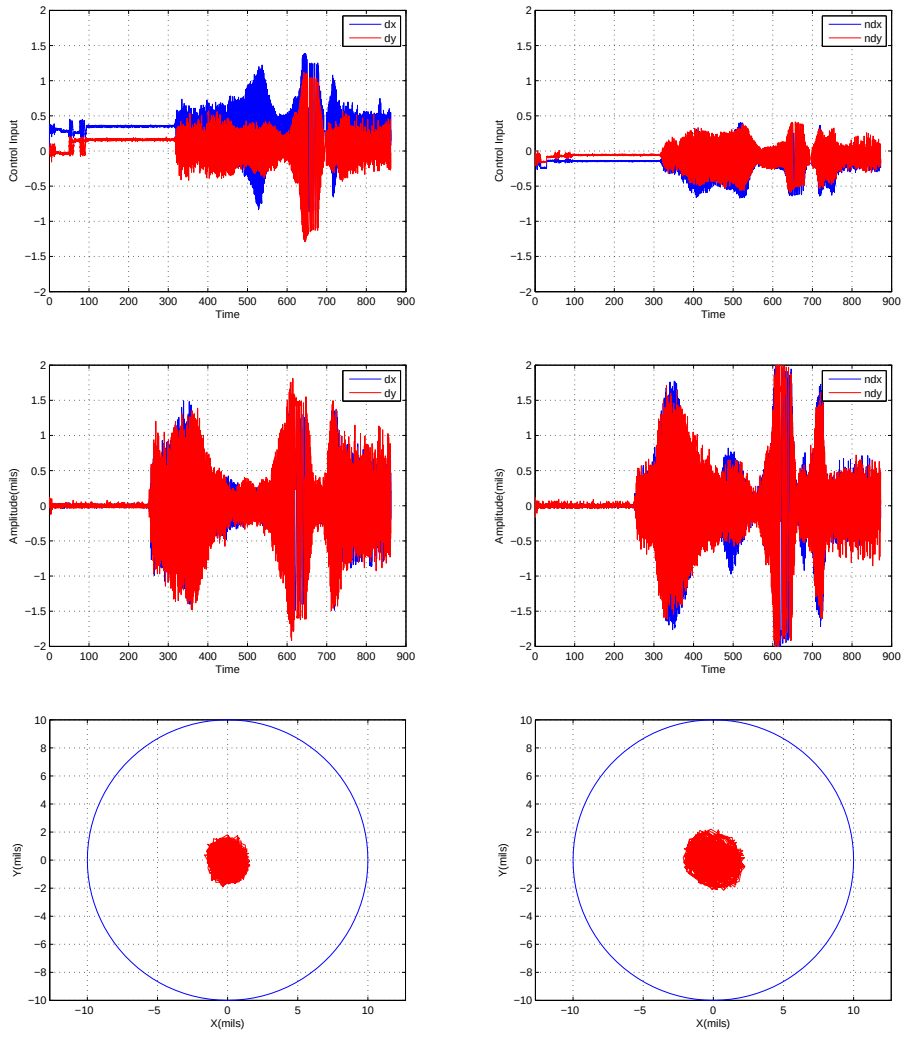

Figure 6: μ-synthesis experimental results (control inputs, shaft displacements and orbit size).

[9] S. E. Mushi. *Robust control of rotordynamic instability in rotating machinery supported by active magnetic bearings*. PhD thesis, Univ. of Virginia, Charlottesville, VA, 2012.

[10] C. Qi, H. Wu, and Z. Lv. The study on the stability of all-coeficient golden section feedback control system. In *Proc. of the 3rd World Congress on Intelligent Control and Automation*, Hefei, China, June 28-July 2, 2000.

[11] H. Wu and Z. Sha. An all-coefficient adaptive control method. *ACTA AUTOMATICA SINICA*, 11(1):12–20, 1985.

[12] B. Meng, H. Wu, Z. Lin, and G. Li. Characteristic model based control of the x-34 reusable launch vehicle in its climbing phase. *Science in China Series F: Information Sciences*, 52(11):2216–2225, 2009.

[13] H. Fujiwara, K. Ebina, K. Ebina, and O. Matsushita. Control of flexible rotors supported by active magnetic bearings. In *Proc. of 8th Int. Symposium on Magnetic Bearings*, pages 145–150, Mito, Japan,

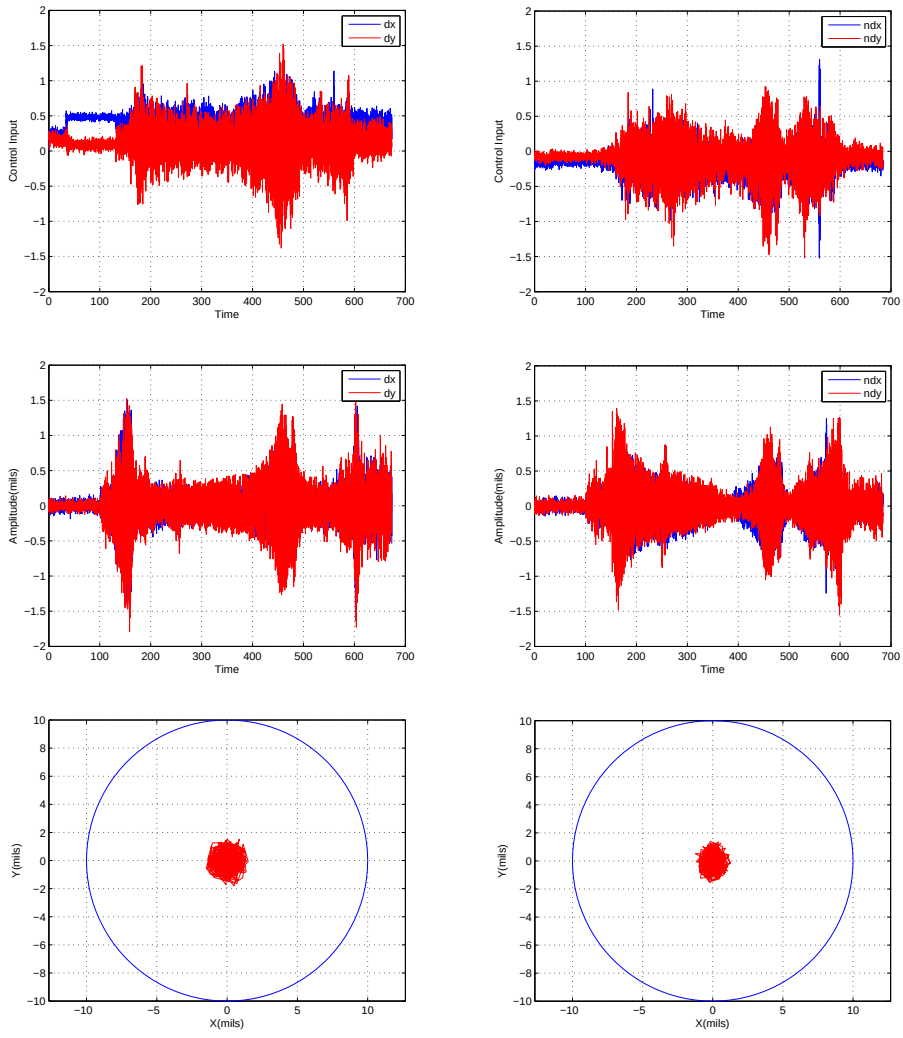

Figure 7: ACAC experimental results (control inputs, shaft displacements and orbit size).

August 26-28, 2002.

[14] S. E. Mushi, Z. Lin, and P. E. Allaire. Design, construction and modeling of a flexible rotor active magnetic bearing test rig. In *Proc. of ASME Turbo Expo 2010: Power for Land, Sea and Air*, Glasgow, UK, June 14-18, 2010.